PNAS RESEARCH ARTICLE | NEUROSCIENCE
PSYCHOLOGICAL AND COGNITIVE SCIENCES OPEN ACCESS

Specialization of the human hippocampal long axis revisited

Peter A. Angeli[a,1], Lauren M. DiNicola[a], Noam Saadon-Grosman[a], Mark C. Eldaief[b], and Randy L. Buckner[a,b,c,1]

Affiliations are included on p. 11.

Edited by May-Britt Moser, Norwegian University of Science and Technology, Trondheim, N/A; received November 4, 2024; accepted December 9, 2024

The hippocampus possesses anatomical differences along its long axis. Here, we explored the functional specialization of the human hippocampal long axis using network-anchored precision functional MRI in two independent datasets (N = 11 and N = 9) paired with behavioral analysis (N = 266 and N = 238). Functional connectivity analyses demonstrated that the anterior hippocampus was preferentially correlated with a cerebral network associated with remembering, while the posterior hippocampus selectively contained a region correlated with a distinct network associated with behavioral salience. Seed regions placed within the hippocampus recapitulated the distinct cerebral networks. Functional characterization of the anterior and posterior hippocampal regions using task data identified and replicated a functional double dissociation. The anterior hippocampal region was sensitive to remembering and imagining the future, specifically tracking the process of scene construction, while the posterior hippocampal region displayed transient responses to targets in an oddball detection task and to transitions between task blocks. These findings suggest an unexpected specialization along the long axis of the human hippocampus with differential responses reflecting the functional properties of the partner cerebral networks.

hippocampus | long Axis | fMRI | memory | salience

Significance

The hippocampus is typically studied in the context of memory and representation of space, while a more limited literature focuses on its role in novelty (salience) detection. Motivated by functional connectivity differences along the long axis of the human hippocampus, we identified subregions that dissociate these functional properties: An anterior hippocampal region is involved in remembering, especially when visualizing a mental scene, while a portion of the posterior hippocampus surprisingly mirrors its partner cerebral network by responding transiently to salient events without any apparent demands on declarative memory. These results suggest that specialization of hippocampal subdivisions can be meaningfully understood by considering how they derive their properties from the brain-wide networks in which they are embedded.

Multiple lines of evidence suggest different possibilities for how the long axis of the hippocampus might be functionally specialized (1, 2). As one example, anchoring from the rich literature on place fields, the dorsal / posterior hippocampus has been implicated in fine-scale spatial representation and navigation (3–10) while the ventral / anterior hippocampus is suggested to support coarser spatial representations (11–14). As another example, building from the association between hippocampal damage and declarative memory deficits (15–18), the anterior hippocampus has been reported to be preferentially involved in memory encoding while the posterior hippocampus is involved in retrieval (19, 20). However, other studies have found minimal effect in the posterior hippocampus (21) or even the opposite specialization (22). These investigations and others (e.g., refs. 23 and 24) support differential specialization along the long axis, but do not agree on a framework to explain the nature of the specialization.

Building on the above work, one approach to understanding long axis specialization examines how hippocampal subregions connect to distinct cerebral networks (e.g., ref. 25). Anatomical tracing studies in nonhuman primates note differential patterns of extrinsic connectivity along the hippocampal long axis (26–28), suggesting that the anterior and posterior hippocampus may be connected to different cerebral networks via the entorhinal cortex. These findings provide context to motivate functional explorations. Specifically, if subregions of the hippocampus are linked to distinct cerebral networks, then functional specializations within the hippocampus might be clarified by exploring response properties related to the specializations of the partner cerebral networks.

Hippocampal-cortical connectivity can be estimated in humans using functional connectivity MRI (29, 30). Functional connectivity from the hippocampus and adjacent parahippocampal cortex reliably includes the retrosplenial / posterior cingulate cortex, caudal posterior parietal cortex, ventromedial prefrontal cortex, dorsolateral prefrontal cortex, and the rostral temporal cortex extending to the pole (e.g., refs. 31–35). The group-averaged human estimate of hippocampal-cortical network organization is similar to the distributed anatomical projection patterns in nonhuman primates (e.g., refs. 36–39; see also ref. 40), reinforcing the potential of a network-anchored approach to functional characterization (despite limitations; see refs. 41–43 for discussion).

In a major advance using within-individual precision neuroimaging, Zheng et al. (44) found that two distinct cerebral networks possess differential coupling to the anterior and posterior hippocampus. The first network, correlated with the anterior hippocampus, is topographically similar to canonical group-based estimates of the hippocampal-cortical network mentioned above and has been functionally associated with autobiographical

Author contributions: P.A.A., L.M.D., M.C.E., and R.L.B. designed research; P.A.A. and L.M.D. performed research; P.A.A., N.S.-G., and R.L.B. analyzed data; and P.A.A. and R.L.B. wrote the paper.

The authors declare no competing interest.

This article is a PNAS Direct Submission.

[1]To whom correspondence may be addressed. Email: peter.a.angeli@dartmouth.edu or randy_buckner@harvard.edu.

This article contains supporting information online at https://www.pnas.org/lookup/suppl/doi:10.1073/pnas.2422083122/-/DCSupplemental.

Published January 14, 2025.

remembering and scene construction, defined by Hassabis and Maguire (45) as the "process of mentally generating or maintaining a complex and coherent scene or event" (e.g., refs. 45–52). This network has also been identified within individuals using high-field fMRI from seed regions placed in the subiculum (53) and parahippocampal area TH (54). By contrast, the posterior hippocampus is correlated with a distinct cerebral network that Zheng et al. (44) described as the Parietal Memory Network (PMN; see ref. 55). This second network includes posterior midline regions that are spatially distinct from the anterior hippocampal network.

Adding nuance to inferring the functions of the hippocampal subregions, the network coupled to the posterior hippocampus includes regions resembling another network extensively studied in the literature, generally referred to as the Salience Network (SAL; refs. 56 and 57). By our estimation, the SAL and PMN networks may be the same network historically described by two different literatures (referred to as SAL / PMN in ref. 52). The observation that the posterior hippocampus may be coupled to a network which responds to transient events raises the possibility that the posterior hippocampus itself may support the detection of salience or novelty (e.g., refs. 58–61). That is, while the field has more often focused on examining hippocampal specialization in relation to spatial and mnemonic processing, the posterior hippocampus' potential linkage to the SAL network suggests a counterintuitive hypothesis: The posterior hippocampus may dissociate from the anterior hippocampus by its response to salient transient events (for background see refs. 56, 57 and 62–64).

With these possibilities in mind, the present work revisits the topic of hippocampal long axis specialization across two independent datasets.

Methods

Overview. The present work explored functional specialization along the long axis of the hippocampus within individuals. Two cohorts of participants were reanalyzed here as independent Discovery (data from ref. 52) and Replication (data from refs. 49 and 50) datasets, with novel focus on the hippocampus. Extending from Zheng et al. (44), resting-state fixation data were first used to estimate differential correlation to cerebral networks along the hippocampal long axis. Then, after identifying anterior and posterior hippocampal regions, functional response properties were examined during a task involving remembering and imagining future scenarios (collectively referred to as "Episodic Projection") as well as tasks targeting low-level oddball detection and transitions between task blocks. All estimates were extracted within the anatomy of individual participants and then averaged afterward to avoid anatomical blurring. A key additional feature of our approach, building from DiNicola et al. (50), was to obtain behavioral assessments of the task strategies employed during the Episodic Projection task trials to further inform the nature of the component processes that drive the hippocampal response. All results were identified in the Discovery Dataset and prospectively replicated in the Replication Dataset; key results were also interrogated using independent methods.

Participants.

Discovery dataset. English-speaking adults ages 18 to 34 without neurological or psychiatric illness completed MRI scanning sessions (data from ref. 52). After quality control exclusions (for details, see *Data Acquisition, Quality Control, and Preprocessing of MRI Data*, as well as *MRI Task Paradigms*), the MRI dataset included 11 participants with a mean age of 22.4 y (SD = 4.1; 11 right-handed; 8 women). Participants were from diverse racial and ethnic backgrounds (7 of 11 individuals self-reported as non-White and/or Hispanic). Behavioral data used to estimate task trial components included, after exclusions for quality control, 266 English-speaking adults located within the United States with high ratings for completion and performance (90%+ approval rating with at least 100 prior tasks approved). Data were collected online through Amazon Mechanical Turk using Cloud Research (65). Behavioral participants had a mean age of 23.2 y (SD = 1.9, 136 women). Discovery MRI participants are labeled P1 to P15 to be consistent with Du et al. (52).

Replication dataset. The independent Replication Dataset included 12 English-speaking adults ages 18 to 25 without neurological or psychiatric illness (data from ref. 49). After quality control exclusions, 9 participants were included (mean age = 21.3 y; SD = 2.1; 8 right-handed; 7 women; 3 non-White / Hispanic). The Replication Dataset also included independent behavioral data collected from 238 participants through Amazon Mechanical Turn via Cloud Research, after screening for quality control (mean age = 22.5 y, Experiment 2 in ref. 50). Replication MRI participants are labeled S7–S18 to be consistent with DiNicola et al. (49).

Participants provided informed consent prior to participation. All procedures for recruitment, consent, and data collection were approved by the Harvard University IRB.

Data Acquisition, Quality Control, and Preprocessing of MRI Data. Scanning was conducted at the Harvard Center for Brain Science using a 3 T Siemens MAGNETOM Prisma^{fit} MRI scanner as described in the study of Du et al. (ref. 52, Discovery Dataset) and that of DiNicola et al. (refs. 49 and 50, Replication Dataset). Key method details are repeated here, for additional information, see *SI Methods*. Data were acquired using a 32- or 64-channel phase-arrayed head coil (Siemens Healthcare, Erlangen, Germany) which were treated as comparable. Discovery Dataset participants completed 8 to 10 neuroimaging sessions with scanning generally completed over 6 to 10 wk, while Replication Dataset participants completed four neuroimaging sessions each. For functional connectivity analyses, 17 to 22 resting-state fixation runs (each 7 min 2 s long) were acquired for each individual in the Discovery Dataset, while 11 fixations runs were acquired in the Replication Dataset. Both datasets also included sequence-matched task runs (*MRI Task Paradigms*).

MRI data were examined for quality prior to analysis (e.g., refs.49 and 66). Run-level exclusion criteria included: 1) maximum absolute motion exceeding 1.8 mm, and 2) closed eyes during skipped or incorrect task trials, or poor task performance. Because each run of the Episodic Projection task as implemented in the Discovery Dataset was significantly longer than other tasks, the maximum absolute motion threshold for this task was raised to 2.5 mm (threshold was kept at 1.8 mm for the Replication Dataset). A full description of participant- and run-level exclusions can be found in *SI Appendix*, Methods. Preprocessing employed an openly available analysis pipeline that aligned data across runs and sessions while minimizing spatial blurring ("iProc", see ref. 53 and *SI Appendix*, Methods).

Cerebral Networks Estimated on the Surface within Individuals. Cerebral networks were identified based on functional connectivity using a multisession hierarchical Bayesian model (MS-HBM) approach computed on the cerebral surface (ref. 67; see ref. 52 for details). Initialized with a 15-network parcellation as a prior, this method results in reliable within-individual estimates of networks by accounting for correlation variability both within an individual and between individuals. To verify the reliability of this parcellation approach, seed-based region correlation was employed to ensure the model-estimated networks were consistent with the underlying distributed correlation patterns (see ref. 52).

Anterior-DN and Posterior-SAL Hippocampal Regions Constructed within Individuals. Within-individual hippocampal regions were defined based on functional connectivity to the two cerebral networks targeted by Zheng et al. (44) (Fig. 1*A*). For each fixation run, the mean BOLD signal was extracted within the Default Network A (DN-A) and Salience / Parietal Memory (SAL / PMN) networks on the cerebral surface and correlated with the BOLD signal within each voxel of each individual's hippocampal boundaries as identified by the automated FreeSurfer parcellation (68, 69). Every voxel along the hippocampus was assigned to the cerebral network with which it was most correlated. Unreliable voxels along the edge of the hippocampal region were excluded, then voxels with a temporal signal-to-noise ratio (SNR) below 50 were removed. Finally, we removed ambiguous voxels with low correlations to both DN-A and SAL / PMN ($z(r) < 0.03$) or with similar correlation values to both cerebral networks, defined as having a normalized correlation difference of less than 0.1 ($|z(r)_{DN\text{-}A} - z(r)_{SAL/PMN}/z(r)_{DN\text{-}A} + z(r)_{SAL/PMN}| < 0.1$, see *SI Appendix*, Table S2 for additional details).

An MNI Y coordinate was chosen as the anterior / posterior border for each individual participant, and voxels assigned to each network were quantified posterior or anterior to that border. The border location was chosen such that the proportion

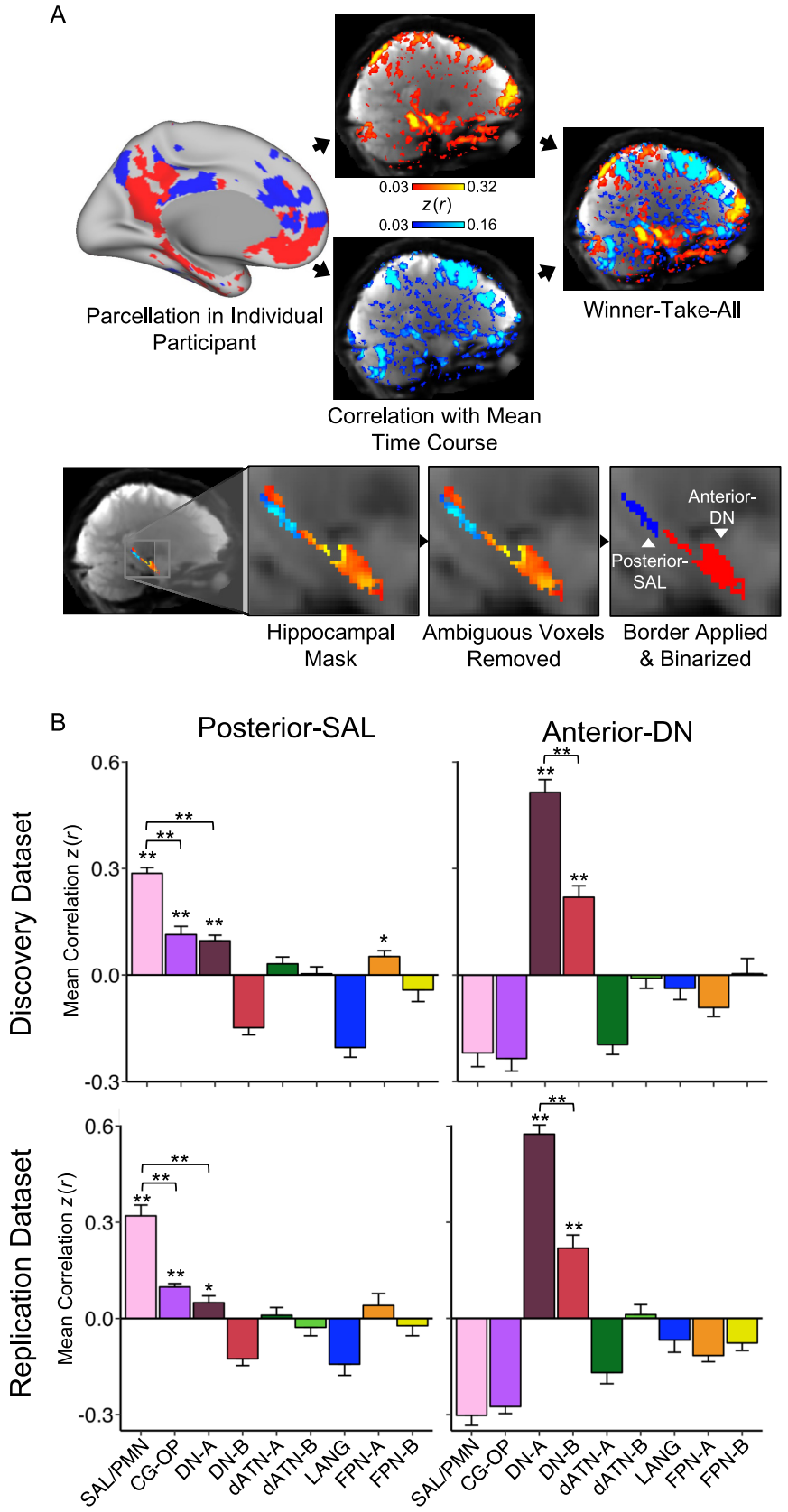

Fig. 1. Posterior-SAL and Anterior-DN hippocampal regions are distinguished by their correlation patterns to distinct cerebral networks. (*A*) In each participant, networks of interest (Default Network A, DN-A, red; Salience Network / Parietal Memory Network, SAL / PMN, blue) were identified on the cortical surface using a multisession hierarchical Bayesian model (MS–HBM). The mean BOLD time-course within each network's boundaries was extracted and correlated with the BOLD time-course of every voxel in the brain volume. Voxels in the volume were assigned to the network with which they were more correlated and masked for the hippocampus after excluding voxels with a signal-to-noise ratio below 50. Within this hippocampal region, ambiguous voxels with comparable correlations to both networks ($|z(r)_{DN\text{-}A} - z(r)_{PMN}/z(r)_{DN\text{-}A} + z(r)_{PMN}| < 0.1$) were removed, and a single network was assigned to define the anterior or posterior region. The network with > 50% of its assigned voxels anterior to border was chosen as the anterior-defining network, while the network with > 50% of assigned voxels posterior to the defined border was chosen as the posterior-defining network. In this representative participant, the border was defined at MNI coordinate Y = −31, and ~84% of DN-A and SAL / PMN voxels defined the anterior and posterior regions, respectively. (*B*) Correlations between hippocampal regions and cerebral networks calculated within an individual were pooled across participants and averaged. In this pooled group average, the Posterior-SAL hippocampal region was significantly correlated with SAL / PMN, CG-OP, and DN-A, with the strongest correlation to SAL / PMN. In contrast, the Anterior-DN hippocampal region was most strongly correlated with DN-A, with a significant but weaker correlation to DN-B. Correlation values are mean Fisher *z*-transformed Pearson's *r* and error bars indicate the SEM *z*(*r*). Networks were clustered using a MS−HBM and labeled according to the convention in ref. 52. SAL / PMN = Salience Network / Parietal Memory Network; CG-OP = Cingulo-Opercular Network; DN-A = Default Network A; DN-B = Default Network B; dATN-A = Dorsal Attention Network A; dATN-B = Dorsal Attention Network B; LANG = Language Network; FPN-A = Frontoparietal Network A; and FPN-B = Frontoparietal Network B. Significance measured with a one-tailed *t* test, H_o: μ = 0, H_a: μ > 0; ** = $P < 0.001$; * = $P < 0.05$

of DN-A assigned voxels in the anterior region (relative to all hippocampal DN-A voxels) and proportion of SAL / PMN assigned voxels in the posterior region (relative to all hippocampal SAL/PMN voxels) would be equal, and vice versa (DN-A proportion posterior to border equal to the SAL / PMN proportion anterior). In practice, this identified the coordinate where, moving along the long axis, one network's assigned voxels began to be more prevalent while the other network's assigned voxels began to be less prevalent. Following border assignment, hippocampal voxels anterior and posterior to the border assigned to the defining network (DN-A or SAL / PMN) were kept for whichever side of the border contained the majority of that network's assigned voxels (voxels on the border were included in the anterior region). Voxels belonging to the nonassigned network were removed, and the remaining voxels were binarized to produce masks for the

hippocampal regions that represented a best estimate of the anterior and posterior regions linked to the two separate cerebral networks. We heuristically label the resulting hippocampal regions Anterior-DN and Posterior-SAL to respect their anatomical location along the long axis of the hippocampus and highlight that they are specifically the subdivisions most correlated with two specific networks.

The selectivity of these regions' functional connectivity to the cerebral cortex was assessed by correlating the BOLD time course within each hippocampal region (whole brain regressed and bandpass filtered, as described in *SI Appendix*, Methods) with the BOLD time course of every vertex on the surface projected data (whole brain regressed, bandpass filtered, and smoothed to 2 mm FWHM). The *z*-transformed correlation maps were visualized on the cerebral surface (*SI Appendix*, Figs. S3–S6). Functional connectivity with a priori identified cerebral networks was quantified by averaging across all the vertices within each network to confirm the linkage of the hippocampal regions with specific distributed cerebral networks (Fig. 1*B*).

Model-Free Seed-Region Based Functional Connectivity. As a control analysis, in the Discovery Dataset, a model free seed-based approach (e.g., refs. 66 and 70) was used to assess the specificity of the functional connectivity to the hippocampus, rather than nearby cortical and subcortical structures. For this exploration, the pair-wise Pearson correlation was calculated between every voxel within an expanded hippocampal mask (59,343 to 68,354 voxels), based on an individual's FreeSurfer parcellation, to every vertex on the cortical surface (81,924 vertices). The resulting correlation matrix was calculated for each resting-state fixation run, Fischer *z*-transformed, and averaged across all fixation runs to yield a single best estimate of that participant's correlation structure. This correlation structure was then explored using Connectome Workbench's wb_view software (71, 72) by interactively choosing cerebral seed regions and visualizing the correlations from that seed region using the Jet look-up table (colorbar), excluding negative values. The correlations were thresholded to best see the functional connectivity topography on the cerebral surface and in the hippocampal volume (*SI Appendix*, Figs. S9–S19).

MRI Task Paradigms. Participants in the Discovery Dataset completed multiple runs of an Episodic Projection task, multiple runs of a Visual Oddball Detection task, and multiple runs of a Blocked Visual-Motor task. The Replication Dataset also included the Episodic Projection Task (see Exp 2 and 3 in ref. 49), along with a blocked Working Memory (N-Back) task. These tasks are described in brief below, for additional details, see *SI Appendix*, Methods, as well as Du et al. (52) and DiNicola et al. (49).

The Episodic Projection task probed processes related to remembering the personal past and imagining the future with multiple-choice questions. Target conditions asked participants to consider scenarios about their past (Past Self) or possible future (Future Self). The Visual Oddball Detection task was designed to assess responses to rare task-relevant visual stimuli (similar to ref. 73). Participants were rapidly presented with upper case "K"s and "O"s in either black or red, and asked to respond only when the target red upper case K was presented (10% of presentations). In the Blocked Visual-Motor task participants viewed discrete blocks of visual flickering checkboards, during which they indicated whether a pair of checks (which appeared 7 to 8 times per block) were near to the center or far from the center. Finally, during the Blocked Working Memory task participants viewed blocks of sequentially presented upper-case consonant letters. For each letter, participants indicated whether that letter matched the letter shown 2 presentations earlier. In both the Blocked Visual-Motor and Blocked Working Memory tasks, task blocks were interspersed with blocks of passive fixation.

Online Behavioral Task Paradigm. The goal of the online behavioral task was to assess the component processes that were embedded within each trial of the scanned Episodic Projection task, extending the procedure of DiNicola et al. (50). The idea motivating the approach is that each trial possesses an idiosyncratic set of features that shape how participants solve the trial, with differences from one trial to the next. Some trials may be more difficult than others, some may rely on scene construction more than others, etc. By assessing strategies used, on average, to complete each unique trial, the behavioral ratings of component processes can provide a means to explore what correlates with the MRI-measured functional responses.

The Episodic Projection task trials were administered to online participants via the Qualtrics survey tool (Qualtrics, Seattle, WA). Given the burden of doing the task and answering multiple strategy questions about each trial, data collection was spread across 10 (Discovery Dataset) or 6 (Replication Dataset) separate cohorts of participants. Online presentation was similar to the scanned task. A few questions required minor wording changes to be applicable to online participants. After answering each individual question, participants reported the cognitive strategies they used when answering the question by giving a number from 1 (not used at all) to 7 (used extensively) for each of 21 strategies (16 strategies in the Replication Dataset). Only after completing this reflection was the participant able to move forward and view the next trial. Strategies collected included 13 shared between both datasets, along with 8 and 3 unique strategies for the Discovery and Replication Datasets, respectively (see *SI Appendix*, *Methods* additional details).

MRI Task Analysis. Task MRI data were analyzed using run-specific general linear models (GLMs) implemented through FSL (version 5.0.4) first-level FEAT (74). Data were high-pass filtered with a cutoff at a period of 100 sec to remove low frequency noise, and GLMs were then run for the cortical surface using whole-brain regressed data (smoothed to 2 mm FWHM) and the entire MNI152-registered volume including the hippocampus (whole-brain regressed, not smoothed). Task contrasts were created separately for each run and averaged across runs to create an average task contrast using *fslmaths* (75). These mean values were extracted within each participant's individualized cerebral networks (from the surface) and the anterior and posterior hippocampal regions (from the volume). Episodic Projection and Visual Oddball tasks were analyzed at the level of conditions, and the Episodic Projection task was subsequently analyzed isolating each trial. Blocked Visual-Motor and Working Memory Tasks were analyzed with a focus on change at block transitions. For full details, see *SI Appendix*, Methods.

Behavioral Task Analysis. The mean trial-level strategy ratings from the online Episodic Projection task were *z*-scored and clustered (hclust function and ward.D2 amalgamation procedure in R) to create robust composite strategy scores for every Episodic Projection task trial. Strategies which clustered together in ref. 50 were also closely clustered in the new Discovery set, again yielding 5 clusters (*SI Appendix*, Fig. S20): I) *Difficulty* (Facts and Difficulty strategies), II) *Scene Construction* (Loc_Obj_Places and Visual_Imagery strategies), III) *Others-Relevant* (Others_Feelings and Other_Personality strategies), IV) *Self-Relevant* (Pers_Feelings and Emotions strategies), and V) *Autobiographical* (Pers_Past_Experiences and Sequence_Events strategies). Trial-level z-scored ratings for strategies in each cluster were summed to produce the "Mean Rating" for each grouping.

Region-Free Hippocampal Exploration. Following our initial analyses using the Anterior-DN and Posterior-SAL hippocampal regions, we explored hippocampal network assignment and task response along the long axis without using a priori regions. This allowed the patterns to be visualized without assumptions about how regions are defined to establish, using convergent methods, that the patterns of network assignment and response generalize across analytic procedures.

For region-free network analysis, all participants across both the Discovery and Replication Datasets were combined to increase power (N = 20). The most correlated network was estimated for every hippocampal voxel, allowing the voxel to be associated with any of the 15 defined networks (as in ref. 70). We then split each individual's hippocampus in 18 segments equally spaced along the MNI Y axis, calculated the proportion of each segment's voxels which were assigned to a given network, and then mean averaged those proportions across individuals to produce a group estimate. The goal of this analysis was to provide another means of visualizing heterogeneity along the long axis of the hippocampus.

Region-free task exploration analyses used the Discovery Dataset, given the availability of the Visual Oddball Detection Task (N = 11). The goal of this analysis was to plot the task response across voxels in the hippocampus using between-participant averaging rather than assuming region boundaries. We mean averaged hippocampal z-scores from the DN-A-regressed GLM (*SI Appendix*, Methods) across participants and masked the result with the binarized average of all participants SNR-screened hippocampal mask.

Results

Regions within the Anterior and Posterior Hippocampus Correlate with Distinct Cerebral Networks. Distinct patterns of functional connectivity were found in the hippocampus from the

cerebral DN-A and SAL / PMN networks. In both the Discovery and Replication datasets, voxels in the anterior hippocampus were nearly all more strongly correlated with DN-A than SAL / PMN, while voxels more correlated with SAL / PMN were found in the posterior hippocampus (*SI Appendix*, Figs. S1 and S2). The effect was not absolute but was present in every participant and robust in most. Across participants the anterior–posterior border, where the relative differential connectivity to one network over the other flipped, fell between MNI Y coordinates −23 and −34, and in all cases DN-A was assigned to the region anterior to this border while SAL / PMN was assigned to the region posterior to the border (*SI Appendix*, Figs. S1 and S2).

Because of the robustness of this anatomical dissociation, we refer to these regions as Anterior-DN and Posterior-SAL, using both their network assignment and anatomical location, but it is important to note that these regions are most accurately thought of as subdivisions of the anterior and posterior hippocampus, or anatomically constrained network assignments. Defining regions based on assignment to a given network follows the example set by functional explorations of networks in the cerebral cortex (e.g., refs. 49–52 and 76) and the cerebellum (e.g., ref. 77). This approach focuses analyses on subregions that are preferentially aligned to distinct networks while minimizing experimenter bias. Investigation of voxel-level network assignment in the hippocampus without anatomical constraints (*SI Appendix*, Figs. S1 and S2) confirms the usefulness of this heuristic in the vast majority of participants and shows its boundaries. Specifically, while DN-A was often found throughout the hippocampus, it was concentrated anteriorly in nearly all participants, while SAL / PMN was uniformly only present posteriorly, although in some participants only slightly.

To explore whether the defined hippocampal regions were preferentially correlated with the targeted networks without imposing strong model assumptions, correlations from the two hippocampal regions were visualized across the entire cerebral surface. While some level of convergence onto the networks used for region definition (DN-A and SAL / PMN) is expected, it is not obligated. For example, a region could show substantial coupling to networks beyond the two used for region definition, or to only subportions of each network. In all participants in both datasets, visual inspection of the pattern of correlations from the hippocampal regions to the cerebral surface suggested strong preferential coupling to the two networks chosen to define each region (*SI Appendix*, Figs. S3–S6). Quantification of correlations both aggregated across all participants (Fig. 1*B*) and examined at the individual level (*SI Appendix*, Figs. S7 and S8) confirmed the preferential connectivity of the hippocampal regions with DN-A and SAL / PMN.

Quantification of hippocampal-cortical correlations also revealed additional details. The Posterior-SAL hippocampal region was most correlated with cerebral SAL / PMN in both datasets (one-sided Student's *t* test, Discovery: $t(10) = 18$, $P < 0.001$; Replication: $t(8) = 9.52$, $P < 0.001$). Significant correlations were also observed to DN-A (Discovery: $t(10) = 6.25$, $P < 0.001$; Replication: $t(8) = 2.3$, $P < 0.05$) and the Cingulo-Opercular Network (CG-OP, Discovery: $t(10) = 4.92$, $P < 0.001$; Replication $t(8) = 9.49$, $P < 0.001$), but these were both weaker than the correlation to SAL / PMN (two-sided Student's paired *t* tests, $P < 0.001$). In contrast, the Anterior-DN hippocampal region was preferentially correlated with DN-A (Discovery: $t(10) = 14.2$, $P < 0.001$; Replication: $t(8) = 20.2$, $P < 0.001$) and to a significantly lesser degree DN-B (Discovery: $t(10) = 6.78$, $P < 0.001$; Replication: $t(8) = 5.37$, $P < 0.001$; two-sided paired *t* tests $P < 0.001$), with no detectable coupling to SAL / PMN. The weaker, but still significant, correlations between the hippocampal regions and networks beyond the two networks initially chosen may suggest additional heterogeneity (see ref. 54 for a recent analysis of DN-B in relation to correlations with the hippocampal formation). With these details in mind, the strong and preferential correlations to DN-A and SAL / PMN from the Anterior-DN and Posterior-SAL hippocampal regions replicated Zheng et al. (44) and provided a basis for detailed task-based functional explorations.

As a control analysis to assess whether the estimates of the hippocampal functional connectivity patterns were affected by BOLD signal bleed from the nearby cerebral cortex (i.e., entorhinal cortex, perirhinal cortex, and parahippocampal cortex) or thalamus, rather than signal within the hippocampus itself, we leveraged the large quantity of resting-fixation in the Discovery Dataset to visualize correlations in the hippocampus from anteromedial and posteromedial cerebral cortical seed regions which reproduced the cerebral network patterns (*SI Appendix*, Figs. S9–S19). Across all participants, both anterior and posterior seed regions in cerebral DN-A converged on correlation peaks within or near the anterior hippocampus that were not continuations of the immediately surrounding cerebral cortex. Seed regions within SAL / PMN produced similarly convergent correlations within the posterior hippocampus, distinct from the nearby parahippocampal cortex or thalamus.

The Anterior-DN Hippocampal Region Responds during Remembering and Imagining the Future. During the Episodic Projection task, the Anterior-DN hippocampal region displayed significant activity when individuals remembered their past (one-sided Student's *t* test, Discovery: $t(10) = 5.27$, $P < 0.001$; Replication: $t(8) = 6.33$, $P < 0.001$) or imagined their future (Discovery: $t(10) = 7.77$ $P < 0.001$; Replication: $t(8) = 5.98$, $P < 0.001$; Fig. 2*A*) relative to the control condition (considering their present). In both the Discovery and Replication Datasets, the Anterior-DN hippocampal region was significantly more active than the Posterior-SAL region (two-sided Student's paired *t* test, Past: Discovery and Replication $P < 0.01$; Future: Discovery and Replication $P < 0.001$). This functional dissociation is also present within the broader cerebral networks associated with these hippocampal regions (DN-A and SAL / PMN, Fig. 2*A*), reproducing the specialization of cerebral DN-A for remembering the past and imagining the future (49, 51, 52).

The Response of the Anterior-DN Hippocampal Region Tracks Scene Construction. The response of the Anterior-DN hippocampal region across Episodic Projection task trials was significantly correlated with the behavioral estimates of scene construction (Fig. 2*B*; Pearson's correlation, Discovery: $r = 0.40$, 95% CI [0.27 0.52], $t(178) = 5.82$, $P < 0.001$; Replication: $r = 0.47$, 95% CI [0.34 0.57], $t(178) = 7.0306$, $P < 0.001$), while the Posterior-SAL hippocampal region showed no significant correlation in the Discovery Dataset and reduced correlation in the Replication Dataset (Fig. 2*B*; Discovery: $r = 0.08$, 95% CI [-0.06 0.23], $t(178) = 1.12$, $P = 0.27$; Replication: $r = 0.32$, 95% CI [0.18 0.44], $P < 0.001$). In both datasets a direct comparison of the Anterior-DN versus Posterior-SAL hippocampal regions revealed a significant region * scene construction interaction (linear mixed effects model, type II Wald F test, Discovery: $F(1,178) = 36.537$, $P < 0.001$; Replication: $F(1,178) = 15.632$, $P < 0.001$). Control analyses, testing previously described relations between cerebral networks and behavioral estimates, verified that the trial-level strategy estimates newly collected here in the Discovery Dataset behaved similar to previously reported results (*SI Appendix*, Figs. S20–S22). Thus, activity within the Anterior-DN hippocampal region tracks scene construction, differentiating its response properties from

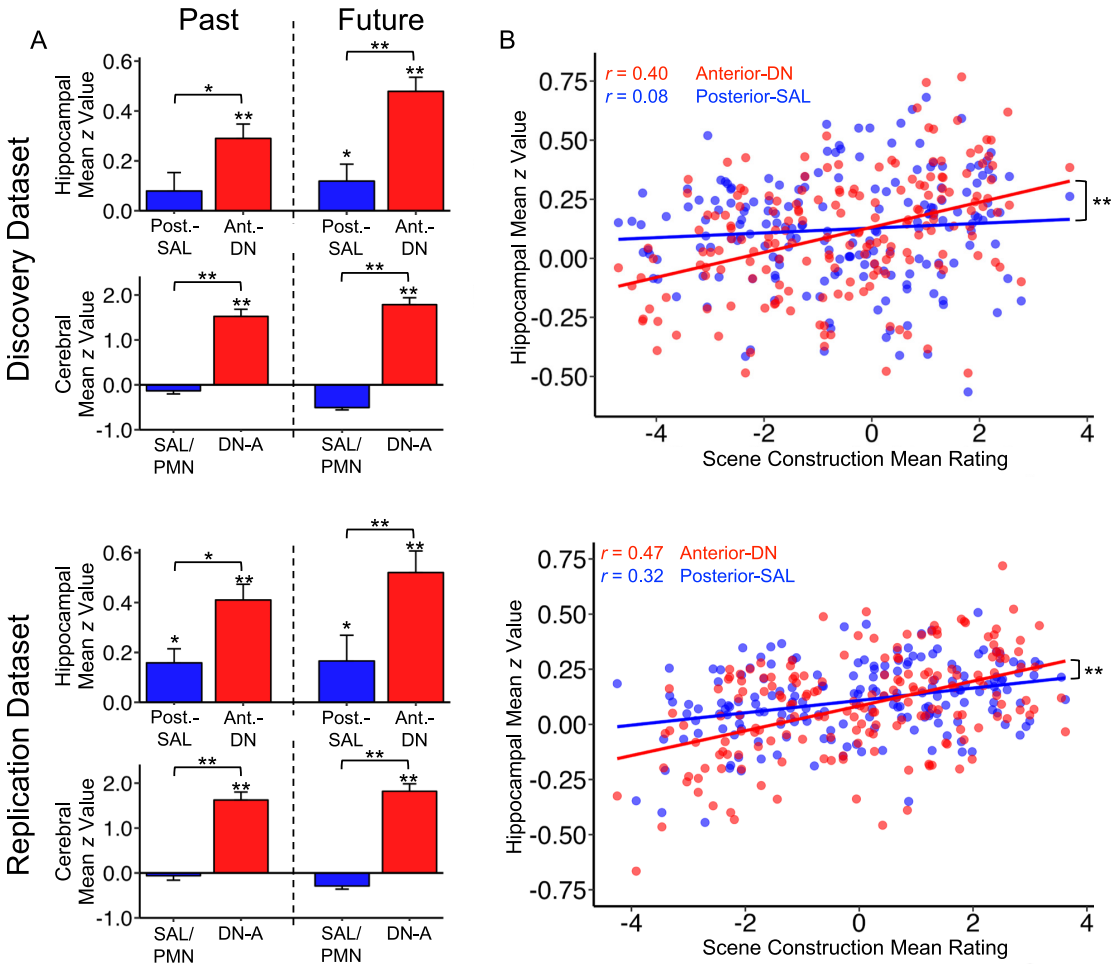

Fig. 2. The Anterior-DN hippocampus responds during remembering and imagining the future and tracks scene construction. Significant effects were found in the initial Discovery Dataset (*Top* panels) and prospectively in the independent Replication Dataset (*Bottom* panels). (*A*) Condition-based analyses of the Episodic Projection tasks reveal increased activity within the Anterior-DN hippocampal region, but not the Posterior-SAL hippocampal region, during contrasts targeting remembering and imagining the future (one-tailed *t* test, H_o: $\mu = 0$, H_a: $\mu > 0$; Past = Past Self – Present Self; Future = Future Self – Present Self). The cerebral DN-A network (below) shows the same pattern, highlighting the similar functional behavior of cerebral DN-A and the Anterior-DN hippocampal region. (*B*) A trial-level behavioral breakdown of activity within the Anterior-DN and Posterior-SAL hippocampal regions reveals (and replicates) that activity within the Anterior-DN hippocampal region is correlated with behavioral scene construction scores (Discovery and Replication: $P < 0.001$), while activity in the Posterior-SAL hippocampus is either not correlated (Discovery: $P = 0.27$) or more weakly correlated (Replication: $P < 0.001$). Both Discovery and Replication Datasets demonstrated a significant region * scene construction interaction ($P < 0.001$). The scene construction score for a given trial is the sum of z-transformed mean ratings for that trial on Loc_Obj_Places and Visual_Imagery strategies. Hippocampal values are mean Fisher *z*-transformed beta values averaged across all participants. Error bars display the SE of the mean. Paired *t* tests are two tailed (H_o: $\mu_1 = \mu_2$, H_a: $\mu_1 \neq \mu_2$). ** = $P < 0.001$; * = $P < 0.05$

the Posterior-SAL hippocampal region in both the Discovery and Replication Datasets.

In their report, Zheng et al. (44) postulated that the anterior hippocampus may be involved in self-relevant processes. The above results suggest scene construction was a significant component process driving the Anterior-DN hippocampal region response in our episodic remembering task (as hypothesized by ref. 78). However, that does not mean the region's response cannot also track component processes related to self-relevance, perhaps reflecting the multiple cerebral networks that are linked to the Anterior-DN hippocampal region (e.g., DN-B; Fig. 1*B*). To explore this possibility, we tested the correlation of our behavioral estimate of self-relevance with the Anterior-DN hippocampal region and found a weaker but still significant correlation in both sets of data (*SI Appendix*, Figs. S23 and S24, Pearson's correlation, Discovery: $r = 0.17$, 95% CI [0.02 0.31], $t(178) = 2.26$, $P < 0.05$, Replication: $r = 0.17$, 95% CI [0.02 0.20], $t(178) = 2.25$ $P < 0.05$). A multiple regression linear model including both scene construction and self-relevance behavioral composites as predictors significantly predicted activity in the Anterior-DN hippocampal region across both datasets (Discovery: $F(2, 177) = 20.2$, $P < 0.001$; Replication: $F(2, 177) = 28.09$, $P < 0.001$), and further showed that scene construction accounted for more variance in the Anterior-DN hippocampal region signal (Discovery: Adjusted $R^2_{\text{Full Model}} = 0.18$, $P_{\text{Scene Construction}} < 0.001$, $P_{\text{Self Relevance}} < 0.05$; $R^2_{\text{Scene Construction}} = 0.16$; $R^2_{\text{Self Relevance}} = 0.02$; Replication: Adjusted $R^2_{\text{Full Model}} = 0.23$, $P_{\text{Scene Construction}} < 0.001$, $P_{\text{Self Relevance}} < 0.05$; $R^2_{\text{Scene Construction}} = 0.21$; $R^2_{\text{Self Relevance}} = 0.02$). Thus, we do find some evidence that the Anterior-DN hippocampal region recruitment tracked self-relevance, but the major association linked to its response was scene construction across both the Discovery and Replication Datasets.

To broadly assess the relative contribution of scene construction versus other component cognitive processes to Anterior-DN hippocampal region activity, we controlled for trial difficulty and fit an additional multiple regression linear model including behavioral composite scores for scene construction and self-relevance, as before, as well as a composite score for autobiographical features

(considering personal past experiences and considering a sequence of events). This difficulty-corrected model continued to significantly predict the Anterior-DN hippocampal region response in both datasets (Discovery: $F(3, 176) = 10.81$, $P < 0.001$; Replication: $F(3,176) = 16.35$, $P < 0.001$). In the Discovery Dataset, only the scene construction composite was a significant predictor (Adjusted $R^2_{\text{Full Model}} = 0.14$, $P_{\text{Scene Construction}} < 0.001$, $P_{\text{Autobiographical}} = 0.13$, $P_{\text{Self Relevance}} = 0.86$), and in the Replication Dataset scene construction remained significant while the autobiographical composite was significant but weaker, and Self Relevance was borderline (Adjusted $R^2_{\text{Full Model}} = 0.20$, $P_{\text{Scene Construction}} < 0.001$, $P_{\text{Autobiographical}} < 0.05$, $P_{\text{Self Relevance}} = 0.05$).

Finally, as an extreme test of the hypothesis that the Anterior-DN hippocampal region responds to the process of scene construction, we restricted our analyses to only control condition trials (Present Self, Past Non-Self, Future Non-Self, and Present Non-Self). Even in these trials, designed to minimize episodic memory demands, activity within the Anterior-DN hippocampal region was significantly correlated with the behavioral estimates of scene construction in the Discovery Dataset (Pearson's correlation, $r = 0.21$, 95% CI [0.03 0.38], $t(118) = 2.36$, $P < 0.05$) and in the Replication Dataset ($r = 0.31$, 95% CI [0.13 0.46], $t(118) = 3.50$, $P < 0.001$). The Anterior-DN hippocampal region was significantly more sensitive to scene construction than the Posterior-SAL hippocampal region in the Discovery Dataset (hippocampal region * scene construction interaction: linear mixed effects model, type II Wald F test, $F(1, 118) = 10.7$, $P < 0.01$). In the Replication Dataset the effect did show a trend but did not reach significance (hippocampal region * scene construction interaction: $F(1, 118) = 2.18$, $P = 0.14$).

The Posterior-SAL Hippocampal Region Transiently Responds during Oddball Detection. We tested the hypothesis that the function of the Posterior-SAL hippocampal region might be understood by anchoring from the role of the SAL / PMN in detecting salient, novel events and responding to task transitions (56, 57, 62–64). We first explored the response of the hippocampal region in the Discovery Dataset with a Visual Oddball Detection task (requiring detection of red Ks among rapidly presented letters). In the cerebral cortex, the set of regions activated by the salient targets included the SAL / PMN network (*SI Appendix*, Fig. S25). Quantification of this response (*SI Appendix*, Fig. S25*C*) confirmed activity to salient targets within the cerebral SAL / PMN (one-sided Student's t test, $t(10) = 5.83$, $P < 0.001$) and closely related CG-OP ($t(10) = 9.92$, $P < 0.001$) networks. Consistent with the dissociation raised in ref. 44, we also observed large decreases in response to salient targets in both the DN-A and DN-B networks (*SI Appendix*, Fig. S25; see also ref. 52). Given these results for the cerebral cortex, we turned our attention to the hippocampal regions, where we observed a prominent functional dissociation that distinguished the response in the posterior from the anterior hippocampus.

Before presenting these results, it is important to touch on the issue of appropriate baselines (for more see ref. 79). Of particular note, the Visual Oddball Detection task produces significant and robust "deactivations" within DN-A consistent with the canonical task-suppression effect common to the "Default Network" (see ref. 80 for discussion). Because the Posterior-SAL hippocampal region defined here possesses voxels that are also correlated with DN-A (Fig. 1*B*), to visualize responses within this region that are above-and-beyond the task suppression effect we applied two methods. The first method compared the Posterior-SAL hippocampal region response to activity within the Anterior-DN hippocampal region to directly assess the differential effect. The second post hoc method regressed out the mean response of cerebral DN-A from the response in the hippocampal regions. This second analysis should be thought of as helping to contextualize a pattern rather than changing a pattern, as it is the relative baseline that shifts.

Both analytical approaches for assessing Posterior-SAL hippocampal region activity revealed a significant response to salient oddball targets (Fig. 3*A*). Post hoc regression with cerebral DN-A uncovered significant positive activation against the relative (regressed) baseline (Fig. 3*A*, right; one-sided Student's t test, $t(10) = 2.8$, $P < 0.05$), and the Posterior-SAL hippocampal region showed significantly greater activation than the Anterior-DN hippocampal region, both with and without regression (two-sided paired Student's t test, without regression: $t(10) = 5.84$, $P < 0.001$; with DN-A regression: $t(10) = 4.64$, $P < 0.001$).

As a final analysis to investigate the posterior hippocampal region's response, activity within the Posterior-SAL hippocampal region was mean averaged after each of the target trials to visualize the evolution of the hemodynamic response (relative to DN-A baseline to overcome the task suppression effect). This procedure allowed visualization of the shape of the transient response time-locked to the oddball events. A robust, canonical transient hemodynamic response was observed (Fig. 3*B*). These results indicate that the Posterior-SAL hippocampal region not only responds transiently to simple salient target stimuli more than the Anterior-DN hippocampal region, but also responds above and beyond the task-suppression baseline effect.

Given the complexities of these analyses and the need for replication, we next sought and found evidence for a transient response in the Posterior-SAL hippocampal region in two independent datasets that employed distinct task paradigms.

The Posterior-SAL Hippocampal Region Transiently Responds at Task Block Transitions. The observation that the Posterior-SAL hippocampal region responds to visual oddball targets, while predicted by the association of the region with the cerebral SAL / PMN network, was nonetheless surprising given there were no declarative or associative memory demands. To generalize this important effect to independent paradigms and expand it to the Replication Dataset, we explored Anterior-DN and Posterior-SAL hippocampal region responses in Blocked Visual-Motor (Discovery) and Blocked Working Memory (Replication) task paradigms that possessed embedded transitions at the beginnings and endings of the task blocks (e.g. refs. 62–64).

Fig. 3 *C* and *D* illustrates the results. At each block transition – including both transitions from visual fixation to the active task block and the reverse transitions going from the active block to passive fixation – there was a transient response observed in the Posterior-SAL hippocampal region that paralleled the block transition effect in the cerebral SAL / PMN network. *SI Appendix*, Figs. S26 and S27 show results both with and without regression of cerebral DN-A activity. While the response in both datasets was largest in the initial transition from fixation to the active task block, it was also clearly present in transitions to the passive fixation blocks, where minimal dynamic task demands are present after the transition.

These results collectively support that the Posterior-SAL hippocampal region responds transiently at task block transitions across independent datasets.

Hippocampal Long Axis Specialization is Revealed by Region-Free Analyses. While the network-derived approach using defined regions proved powerful for identifying and characterizing functionally specialized regions of the anterior and posterior hippocampus, it imposes assumptions. Specifically, exploring only

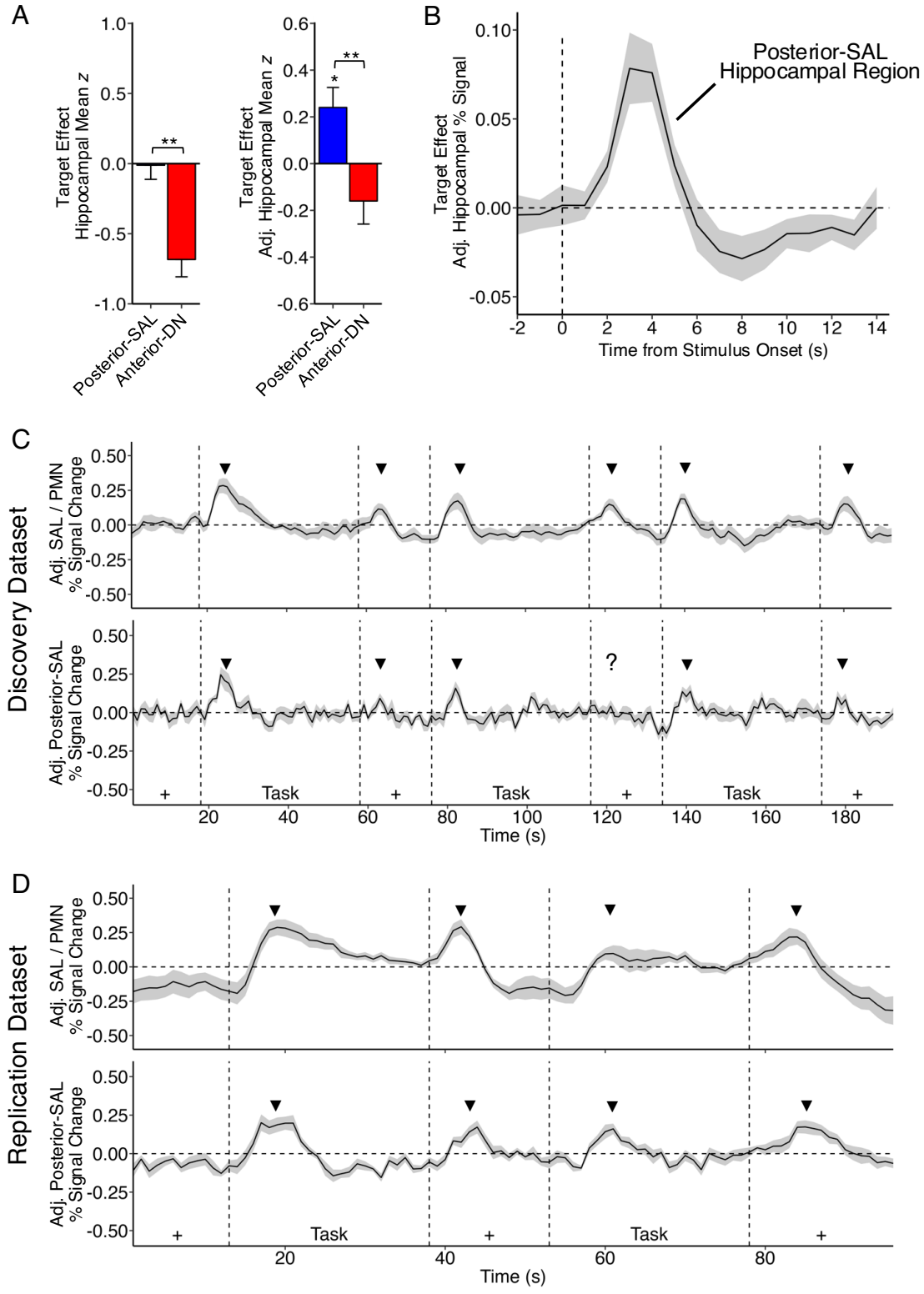

Fig. 3. The Posterior-SAL hippocampus transiently responds to oddball targets and task transitions. Significant effects were found across three independent datasets. (*A*) Within the hippocampus, the Posterior-SAL region is significantly more active than the Anterior-DN region in response to Visual Oddball task salient targets, although both display relatively low activity (meaning the reference baseline is high). Regressing DN-A activity from both hippocampal regions shifts the baseline. (*B*) Plotting the adjusted mean percent signal change within the Posterior-SAL hippocampal region time locked to the target oddball events shows a transient, canonical hemodynamic response. The dashed line shows the onset time of the targets. The shading around the response indicates the SEM. (*C*) Adjusted time courses for the Blocked Visual-Motor task. Discovery data are shown for the cerebral SAL / PMN network (*Top*) and for the Posterior-SAL hippocampal region (*Bottom*). The dashed lines indicate the transitions between blocks with the notation at the bottom indicating the block types (Task or fixation, +). The arrows indicate the transient responses at the block transitions. (*D*) Adjusted time courses for the Blocked Working Memory task data are plotted similarly to demonstrate the effects replicate in an independent dataset. Significance statistics are either a one-tailed *t* test for each hippocampal region (H_o: $\mu = 0$, H_a: $\mu > 0$), or a two-tailed paired *t* test to assess for differences between the hippocampal regions (H_o: $\mu_1 = \mu_2$, H_a: $\mu_1 \neq \mu_2$). Error bars indicate SEM. ** = $P < 0.001$; * = $P < 0.05$

two networks ignores possible influences from other networks and requires a binarization along the long axis, whereas actual functional specialization could involve other networks or be better represented by a gradient.

To address these issues, we characterized how network connectivity and task activation varied along the hippocampal long axis in a continuous manner rather than using network-defined regions (Fig. 4). This analysis showed that hippocampal voxels preferentially correlated to only a small subset of cerebral networks: DN-A, SAL / PMN, DN-B, and FPN-B. Of these, DN-A and SAL / PMN demonstrated the most pronounced differences along the long axis. FPN-B showed a small number of correlated voxels along the entire long axis, while DN-B voxels were a minority in the anterior hippocampus before disappearing as one moves posteriorly. Both these correlations will require further study beyond the present work.

For our a priori networks of interest, DN-A and SAL / PMN, the model-free analysis confirmed at the group level the pattern observable in our participant-specific analyses (*SI Appendix*, Figs. S1 and S2): correlation to DN-A is broadly present in many voxels throughout the long axis of the hippocampus, though generally higher in the anterior hippocampus, while SAL / PMN correlated voxels emerge around the midpoint of the hippocampus and steadily increase toward the tail, eventually becoming as prevalent as DN-A.

We further sought to clarify the surprising result showing sensitivity to transient, salient events within the Posterior-SAL hippocampal region by calculating the mean response to salient targets throughout the entire extent of the hippocampus (after regressing cerebral DN-A activity, Fig. 4*B*). This final analysis confirmed that the posterior hippocampus generally shows a qualitatively different response from the anterior hippocampus, as predicted by the regional analyses (Fig. 3*A*).

Thus, by all analysis approaches across multiple datasets and task paradigms, the posterior hippocampus possesses a region showing sensitivity to novelty and transient events in a manner that is functionally dissociated from responses in the anterior hippocampus.

Discussion

The anterior hippocampal region, like its partner cerebral network, responds during remembering and imagining the future, tracking the process of scene construction – a core component of episodic memory linked to hippocampal function (45, 78). By contrast, the posterior hippocampal region, like its partner cerebral network, responds transiently during oddball detection and also at the transitions between task blocks. This salience effect was replicable across datasets and found through analysis of multiple distinct paradigms. The response of the posterior hippocampal region to oddball targets and task transitions is present despite the absence of declarative or associative memory demands, and is present in a large portion of the anatomically defined posterior hippocampus. While network-level dissociations have been observed from careful anatomical tracing in nonhuman primates (26–28) and previous fMRI work (25, 31), the identification and replication of a response to salient events in the posterior hippocampus which can be dissociated from the anterior hippocampus may reconcile disparate hypotheses about hippocampal function.

The Anterior Hippocampus Tracks Scene Construction during Remembering and Imagining the Future. Our estimates, like those of Zheng et al. (44), reveal that an anterior hippocampal region is preferentially correlated with the distributed cerebral

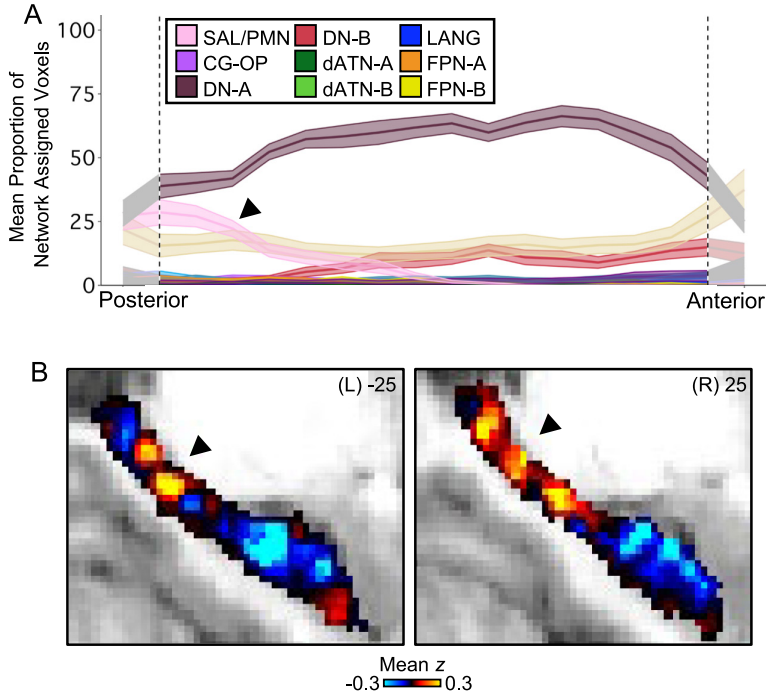

Fig. 4. Region-free analyses support posterior hippocampal coupling to SAL / PMN and response to oddball targets. (*A*) Mean voxel-level network assignments along the hippocampal long axis confirm significant coupling to SAL / PMN in the posterior hippocampus (indicated by arrow) along with a relative decrease in coupling to DN-A. Note that while couplings to DN-A and SAL / PMN are the most prominent network assignments across the hippocampal long axis, there is also lesser correlation to other networks including DN-B and FPN-B. Shading around the lines indicates the SEM. The vertical dashed lines demarcate shaded portions of the most posterior and anterior regions where the data are ambiguous due to low voxel counts. (*B*) The anterior and posterior hippocampus display differential responses to Visual Oddball salient targets. Specifically, the posterior portions of the hippocampus show increased activity to oddballs (hot colors), while the anterior hippocampus displays decreased activity (cool colors). Note that this analysis is not constrained by a priori definition of regions. The map displays the group mean average *z*-value map after regressing cerebral DN-A activity (*SI Appendix*, Methods) on an individual anatomical scan for reference. Arrows indicate the posterior regions of the hippocampus that display a transient positive response.

network historically referred to as the Default Network. This region is most strongly correlated with DN-A (Fig. 1*B*), leading to our prediction that the Anterior-DN hippocampal region might track the process of scene construction (45, 50, 78). This prediction was borne out and replicated.

The Anterior-DN hippocampal region was significantly active during remembering the past and imagining the future, and more so in both conditions as contrasted with the Posterior-SAL hippocampal region (Fig. 2*A*). Moreover, the response in the Anterior-DN hippocampal region across trials demonstrated a reliable association with the component process of scene construction (Fig. 2*B*). This relation with scene construction was inconsistent for the Posterior-SAL hippocampal region but was present in the Anterior-DN region even during control trials, suggesting anatomical and functional specificity (*SI Appendix*, Figs. S23 and S24).

Thus, consistent with observations by others (45, 78, 81, 82), portions of the hippocampus track the component process of scene construction. The hippocampus has long been shown to be involved in spatial processing in both rodents (6, 7) and humans (e.g., refs. 3–5 and 8), but this function has largely been localized to the dorsal / posterior hippocampus. The present results reveal a replicable association of the human anterior hippocampus with scene construction.

Our results are consistent with recent work, building on the observation of a hippocampal representational gradient of space (11, 12), implicating the anterior hippocampus in initial, coarse scene construction with the posterior hippocampus activated by distinct task components (83, 84). In our data, the anterior region reproducibly tracked constructive aspects of scene construction, and critically was functionally dissociated from a region within the posterior hippocampus. The nature of the response in the posterior hippocampus was revealed by examining its response to transient, salient events.

The Posterior Hippocampus Responds to Salient Transients. A surprising but clear finding is the transient response within the posterior hippocampus to oddball targets and transitions between task blocks (Fig. 3). The motivation to explore such processes was drawn directly from the cerebral network estimated to be linked to the posterior hippocampus. In this regard, our interpretation of the network correlation pattern for the Posterior-SAL hippocampal region differs from that of Zheng and colleagues (44). We hypothesize the major network correlated with the Posterior-SAL hippocampal region is the same as the network described by Seeley and colleagues as the "Salience Network" (SAL; refs. 56 and 57; see also ref. 62), with weaker coupling to the nearby and closely related Cingulo-Opercular Network (CG-OP; refs. 56 and 62). In contrast, Zheng and colleagues proposed that the posterior hippocampal network is linked to memory functions through a sensitivity to familiarity. The basis of their hypothesis is prior studies that have demonstrated regional responses at and around the PMN to item repetitions in memory paradigms (e.g., ref. 55; see also refs. 85 and 86).

Our alternative interpretation, based on the observation that the primary posterior hippocampal network is spatially similar to the SAL network (see ref. 52 for discussion), led us down a different path. We hypothesized and found evidence that the Posterior-SAL hippocampal region responds to oddball targets and task transitions. The effect replicated across two datasets involving two distinct tasks, analyzed in relation to both oddball events and task transitions to and away from active tasks. Most surprisingly, the effect was present during tasks absent any traditional declarative or associative memory demands.

These findings are consistent with work describing a role for the hippocampus in processing surprise or novelty (e.g., refs. 58–61). In our paradigms transient responses were noted both to isolated, repeating simple letter stimuli when they were oddball targets and at task block transitions, including when the transition was away from an active task and toward passive fixation. Previous neuroimaging investigations have noted transient responses in the hippocampus at the borders between complex, meaningful stimuli such as movies (e.g., refs. 87–91, see also ref. 92), a response often hypothesized to support consolidation.

Here, transient responses were observed in paradigms with no obvious declarative or associative memory demands or meaningful materials to be encoded – just salient stimuli and transitions that required a task set change or orienting response. The oddball task additionally does not seem to include notable event boundaries, beyond possibly the onset and offset of target letters. Our results connect the work on hippocampal novelty responses to the literature on cerebral salience processing (e.g., refs. 56, 57 and 62) and motivate further study of the posterior hippocampus in this context. It is an open question whether the transient responses found here reflect a mechanism that is critical to memory or whether they reveal a processing role of the hippocampus that might best be conceived outside of the traditional focus on declarative memory.

Limitations and Future Directions. The present work contributes to the ongoing debate over the nature of functional specialization within the hippocampus but does not resolve all dimensions of the debate. Our tools and approach are poorly suited to explain and predict activity on the level of cells (e.g., ref. 93) due to the resolution of current neuroimaging methods. Our study also lacks tasks with an encoding-retrieval design, so we cannot address the proposed dissociations along such dimensions (19, 20). We provide positive evidence for a robust double dissociation between subregions of the hippocampus processing space and salience. This functional-anatomical dissociation leaves open the question of how such processing components relate to mnemonic functions, other than noting the process of scene construction is called upon during acts of remembering.

The present work defined hippocampal regions using a combination of functional connectivity-based network assignments and anatomical constraints along the long axis. This approach was chosen a priori to give the best chance of capturing functional dissociations while minimizing experimenter bias and improving interpretability with the larger literature on hippocampal long axis functional dissociations. Our approach resulted in the exclusion of voxels in the posterior hippocampus more coupled to DN-A than SAL / PMN (*SI Appendix*, Figs. S1 and S2), and thus necessarily de-emphasized functional complexity and variability in the posterior hippocampus. To partially mitigate this issue, we explored the organization of the long axis of the hippocampus without strong assumptions or a priori exclusion of networks (Fig. 4). The results revealed that our focus on two networks is warranted and captures the major component networks. However, the results also reveal additional network contributions and complexity in their anatomical distribution. Thus, while capturing critical elements of specialization, the present results do not necessarily explain all dimensions and complexities of hippocampal specialization.

Despite the improvements made possible by adopting a within-individual, network-based approach, our exploration of the hippocampus was limited by technical considerations. First among these is signal dropout in the most anterior portions of the hippocampus and surrounding cerebral regions. Beyond

preventing the inclusion of these regions in our analyses (via screening for tSNR), the lack of signal in regions of the anterior parahippocampal gyrus makes it difficult to assess the possibility of signal bleed from this portion of the cortex, or the amygdala, into included regions of the anterior hippocampus. It is possible that anterior parahippocampal or entorhinal cortex activity, which we are unable to reliably measure, is contributing to responses within the anterior hippocampus. In addition to dropout, the resolution of our BOLD acquisition (2.4 mm isotropic) results in ambiguity around the spatial location of activations and correlations (*SI Appendix*, Figs. S9-S19). The limited resolution also impairs our ability to explore subfield-level network coupling and functional specialization. Future work will benefit from acquisitions at high field with higher resolution to address these issues (e.g., refs. 54 and 94).

A specific future direction of study concerns possible additional relations to processing outside of the spatial domain. The positive evidence presented here for a role of the anterior hippocampus in scene construction should not be taken to mean the region only responds to such processes. Detailed analyses of the correlation of the Anterior-DN hippocampal region to cortex provided evidence for linkage to the DN-B cerebral network (Fig. 1*B*), including in many of the individual participants (*SI Appendix*, Figs. S7 and S8). This association was also present outside our defined region (Fig. 4*A*). Reznik and colleagues (54), using high-field MRI, recently demonstrated that anterior regions of the hippocampal formation, particularly a region within or near to the entorhinal cortex, were linked to the cerebral DN-B network. Future explorations at high resolution are warranted to dig deeper, especially in relation to processing within the social domain linked to the DN-B cerebral network.

Another future direction is to directly explore the relation of the posterior hippocampal transient responses observed here with memory repetition effects that have been the emphasis of prior work on the cerebral SAL / PMN network (and a proposed processing function of the posterior hippocampus; refs. 44, 55, 86 and 94; see also ref. 95). It is notable that maps of repetition effects can look remarkably similar to the visual oddball detection effects observed here. For example, the individual participant maps of repetition effects in the study of Kwon et al. (ref. 94; their Figure. 8, see S3 and S6) are highly similar to the individual participant oddball detection effect maps in the present work (*SI Appendix*, Fig. S25, see P3 and P6).

There are multiple possible ways the two sets of findings might relate. One possibility is that repeating targets in certain forms of recognition or incidental memory paradigms might make the repeated targets more salient. Response times tend to be faster to old items in old / new recognition decisions and confidence goes up with the number of repetitions. Thus, one avenue for future exploration is to explore old / new recognition memory and item repetitions in classic paradigms alongside ones that explicitly shift the relevance of the repetition (e.g., press only to old items or press only to new items; ref. 96). More broadly, it will be interesting to explore processing models that link novelty and detection of salience to memory.

Conclusions

The hippocampus can be robustly dissociated along the long axis based on connectivity to cerebral networks. The Anterior-DN hippocampal region is correlated with the cerebral network DN-A, while the Posterior-SAL hippocampal region is correlated with the cerebral network SAL / PMN. The network-defined Anterior-DN and Posterior-SAL regions display a functional double dissociation, highlighting the value of network-driven, domain-agnostic explorations of hippocampal function. The Anterior-DN hippocampal region is sensitive to remembering, tracking the component process of scene construction; the Posterior-SAL hippocampal region responds transiently to salient stimuli and task transitions.

Data, Materials, and Software Availability. Previously published data were used for this work (49, 52). Network parcellation was performed using code from Kong et al. (67) available on Github (https://github.com/ThomasYeoLab/CBIG/tree/master/stable_projects/brain_parcellation/Kong2019_MSHBM) with a 15-network prior [as in Du et al. (52)].

ACKNOWLEDGMENTS. We thank the Harvard Center for Brain Science neuroimaging core and FAS Division of Research Computing for providing critical support, specifically T. O'Keefe for assisting with data processing optimization and R. Mair for MRI physics support. We also thank J. Du, H. Kosakowski, W. Sun, and M. Elliot for their valuable input and discussions. A. Song, A. Youssoufian, B. Braams, C. Vidal Bustamante, F. Davy-Falconi, H. Becker, K. Miclau, K. Ntoh, and T. Moran assisted with MRI data acquisition. O.I. Ariyo and S. Murdock assisted with online behavioral data acquisition. The multiband EPI sequence was generously provided by the Center for Magnetic Resonance Research at the University of Minnesota, and E. Fedorenko, T. Konkle, and R. Saxe generously provided task stimuli. P.A.A. thanks Daniel Schacter, Rick Born, and Mark Andermann for valuable insights as this work evolved. Supported by NIH grant MH124004, NIH Shared Instrumentation grant S10OD020039, and NSF grant 2024462. L.M.D. was supported by NSF Graduate Research Fellowship Program grant DGE1745303. Any opinions, findings, and conclusions or recommendations expressed in this material are those of the authors and do not necessarily reflect the views of the NSF.

Author affiliations: [a]Department of Psychology, Center for Brain Science, Harvard University, Cambridge, MA 02138; [b]Department of Psychiatry, Massachusetts General Hospital, Charlestown, MA 02129; and [c]Athinoula A. Martinos Center for Biomedical Imaging, Massachusetts General Hospital, Charlestown, MA 02129

1. J. Poppenk, H. R. Evensmoen, M. Moscovitch, L. Nadel, Long-axis specialization of the human hippocampus. *Trends Cogn. Sci.* **17**, 230–240 (2013).
2. B. A. Strange, M. P. Witter, E. S. Lein, E. I. Moser, Functional organization of the hippocampal longitudinal axis. *Nat. Rev. Neurosci.* **15**, 655–669 (2014).
3. E. A. Maguire, R. S. J. Frackowiak, C. D. Frith, Recalling routes around London: Activation of the right hippocampus in taxi drivers. *J. Neurosci.* **17**, 7103–7110 (1997).
4. E. A. Maguire *et al.*, Knowing where and getting there: A human navigation network. *Science* **280**, 921–924 (1998).
5. E. A. Maguire *et al.*, Navigation-related structural change in the hippocampi of taxi drivers. *Proc. Natl. Acad. Sci. U.S.A.* **97**, 4398–4403 (2000).
6. J. O'Keefe, Place units in the hippocampus of the freely moving rat. *Exp. Neurol.* **51**, 78–109 (1976).
7. J. O'Keefe, J. Dostrovsky, The hippocampus as a spatial map. Preliminary evidence from unit activity in the freely-moving rat. *Brain Res.* **34**, 171–175 (1971).
8. L. Ryan, C.-Y. Lin, K. Ketcham, L. Nadel, The role of medial temporal lobe in retrieving spatial and nonspatial relations from episodic and semantic memory. *Hippocampus* **20**, 11–18 (2010).
9. K. Woollett, E. A. Maguire, Acquiring "the Knowledge" of London's layout drives structural brain changes. *Curr. Biol.* **21**, 2109–2114 (2011).
10. K. Woollett, E. A. Maguire, Exploring anterograde associative memory in London taxi drivers. *Neuroreport* **23**, 885–888 (2012).
11. I. K. Brunec *et al.*, Multiple scales of representation along the hippocampal anteroposterior axis in humans. *Curr. Biol.* **28**, 2129–2135.e6 (2018).
12. M. Hirshhorn, C. Grady, R. S. Rosenbaum, G. Winocur, M. Moscovitch, Brain regions involved in the retrieval of spatial and episodic details associated with a familiar environment: An fMRI study. *Neuropsychologia* **50**, 3094–3106 (2012).
13. M. W. Jung, S. I. Wiener, B. L. McNaughton, Comparison of spatial firing characteristics of units in dorsal and ventral hippocampus of the rat. *J. Neurosci.* **14**, 7347–7356 (1994).
14. K. B. Kjelstrup *et al.*, Finite scale of spatial representation in the hippocampus. *Science* **321**, 140–143 (2008).
15. W. B. Scoville, B. Milner, Loss of recent memory after bilateral hippocampal lesions. *J. Neurol. Neurosurg. Psychiatry* **20**, 11–21 (1957).
16. B. Milner, S. Corkin, H.-L. Teuber, Further analysis of the hippocampal amnesic syndrome: 14-year follow-up study of H.M. *Neuropsychologia* **6**, 215–234 (1968).
17. S. Zola-Morgan, L. R. Squire, D. G. Amaral, Human amnesia and the medial temporal region: Enduring memory impairment following a bilateral lesion limited to field CA1 of the hippocampus. *J. Neurosci.* **6**, 2950–2967 (1986).

18. N. J. Cohen, H. Eichenbaum, *Memory, Amnesia, and the Hippocampal System* (MIT Press, 1993).
19. M. Lepage, R. Habib, E. Tulving, Hippocampal PET activations of memory encoding and retrieval: The HIPER model. *Hippocampus* **8**, 313–322 (1998).
20. J. Poppenk, M. Moscovitch, A hippocampal marker of recollection memory ability among healthy young adults: Contributions of posterior and anterior segments. *Neuron* **72**, 931–937 (2011).
21. J. Spaniol *et al.*, Event-related fMRI studies of episodic encoding and retrieval: Meta-analyses using activation likelihood estimation. *Neuropsychologia* **47**, 1765–1779 (2009).
22. D. L. Schacter, A. D. Wagner, Medial temporal lobe activations in fMRI and PET studies of episodic encoding and retrieval. *Hippocampus* **9**, 7–24 (1999).
23. S. H. P. Collin, B. Milivojevic, C. F. Doeller, Memory hierarchies map onto the hippocampal long axis in humans. *Nat. Neurosci.* **18**, 1562–1564 (2015).
24. M. Ritchey, M. E. Montchal, A. P. Yonelinas, C. Ranganath, Delay-dependent contributions of medial temporal lobe regions to episodic memory retrieval. *eLife* **4**, e05025 (2015).
25. C. Ranganath, M. Ritchey, Two cortical systems for memory-guided behaviour. *Nat. Rev. Neurosci.* **13**, 713–726 (2012).
26. D. G. Amaral, M. P. Witter, The three-dimensional organization of the hippocampal formation: A review of anatomical data. *Neuroscience* **31**, 571–591 (1989).
27. R. Insausti, D. G. Amaral, Entorhinal cortex of the monkey: IV. Topographical and laminar organization of cortical afferents. *J. Comp. Neurol.* **509**, 608–641 (2008).
28. M. P. Witter, D. G. Amaral, The entorhinal cortex of the monkey: VI. Organization of projections from the hippocampus, subiculum, presubiculum, and parasubiculum. *J. Comp. Neurol.* **529**, 828–852 (2021).
29. B. Biswal, F. Zerrin Yetkin, V. M. Haughton, J. S. Hyde, Functional connectivity in the motor cortex of resting human brain using echo-planar MRI. *Magn. Reson Med.* **34**, 537–541 (1995).
30. M. D. Fox, M. E. Raichle, Spontaneous fluctuations in brain activity observed with functional magnetic resonance imaging. *Nat. Rev. Neurosci.* **8**, 700–711 (2007).
31. A. J. Barnett *et al.*, Intrinsic connectivity reveals functionally distinct cortico-hippocampal networks in the human brain. *PLoS Biol.* **19**, e3001275 (2021).
32. L. E. Frank, C. R. Bowman, D. Zeithamova, Differential functional connectivity along the long axis of the hippocampus aligns with differential role in memory specificity and generalization. *J. Cogn. Neurosci.* **31**, 1958–1975 (2019).
33. M. D. Greicius, G. Srivastava, A. L. Reiss, V. Menon, Default-mode network activity distinguishes Alzheimer's disease from healthy aging: Evidence from functional MRI. *Proc. Natl. Acad. Sci. U.S.A.* **101**, 4637–4642 (2004).
34. I. Kahn, J. R. Andrews-Hanna, J. L. Vincent, A. Z. Snyder, R. L. Buckner, Distinct cortical anatomy linked to subregions of the medial temporal lobe revealed by intrinsic functional connectivity. *J. Neurophysiol.* **100**, 129–139 (2008).
35. J. L. Vincent *et al.*, Coherent spontaneous activity identifies a hippocampal-parietal memory network. *J. Neurophysiol.* **96**, 3517–3531 (2006).
36. R. L. Buckner, J. R. Andrews-Hanna, D. L. Schacter, The brain's default network: Anatomy, function, and relevance to disease. *Ann. NY Acad. Sci.* **1124**, 1–38 (2008).
37. J. R. Binder, R. H. Desai, W. W. Graves, L. L. Conant, Where is the semantic system? A critical review and meta-analysis of 120 functional neuroimaging studies *Cereb. Cortex* **19**, 2767–2796 (2009).
38. D. S. Margulies *et al.*, Precuneus shares intrinsic functional architecture in humans and monkeys. *Proc. Natl. Acad. Sci. U.S.A.* **106**, 20069–20074 (2009).
39. R. L. Buckner, D. S. Margulies, Macroscale cortical organization and a default-like apex transmodal network in the marmoset monkey. *Nat. Commun.* **10**, 1976 (2019).
40. G. J. Blatt, D. N. Pandya, D. L. Rosene, Parcellation of cortical afferents to three distinct sectors in the parahippocampal gyrus of the rhesus monkey: An anatomical and neurophysiological study. *J. Comp. Neurol.* **466**, 161–179 (2003).
41. R. L. Buckner, F. M. Krienen, B. T. T. Yeo, Opportunities and limitations of intrinsic functional connectivity MRI. *Nat. Neurosci.* **16**, 832–837 (2013).
42. K. Murphy, R. M. Birn, P. A. Bandettini, Resting-state fMRI confounds and cleanup. *Neuroimage* **80**, 349–359 (2013).
43. J. D. Power, B. L. Schlaggar, S. E. Petersen, Studying brain organization via spontaneous fMRI signal. *Neuron* **84**, 681–696 (2014).
44. A. Zheng *et al.*, Parallel hippocampal-parietal circuits for self- and goal-oriented processing. *Proc. Natl. Acad. Sci. U.S.A.* **118**, e2101743118 (2021).
45. D. Hassabis, E. A. Maguire, Deconstructing episodic memory with construction. *Trends Cogn. Sci.* **11**, 299–306 (2007).
46. E. Svoboda, M. C. McKinnon, B. Levine, The functional neuroanatomy of autobiographical memory: A meta-analysis. *Neuropsychologia* **44**, 2189–2208 (2006).
47. D. L. Schacter, D. R. Addis, R. L. Buckner, Remembering the past to imagine the future: The prospective brain. *Nat. Rev. Neurosci.* **8**, 657–661 (2007).
48. J. R. Andrews-Hanna, R. Saxe, T. Yarkoni, Contributions of episodic retrieval and mentalizing to autobiographical thought: Evidence from functional neuroimaging, resting-state connectivity, and fMRI meta-analyses. *Neuroimage* **91**, 324–335 (2014).
49. L. M. DiNicola, R. M. Braga, R. L. Buckner, Parallel distributed networks dissociate episodic and social functions within the individual. *J. Neurophysiol.* **123**, 1144–1179 (2020).
50. L. M. DiNicola, O. I. Ariyo, R. L. Buckner, Functional specialization of parallel distributed networks revealed by analysis of trial-to-trial variation in processing demands. *J. Neurophysiol.* **129**, 17–40 (2023).
51. L. M. DiNicola, W. Sun, R. L. Buckner, Side-by-side regions in dorsolateral prefrontal cortex estimated within the individual respond differentially to domain-specific and domain-flexible processes. *J. Neurophysiol.* **130**, 1602–1615 (2023).
52. J. Du *et al.*, Organization of the human cerebral cortex estimated within individuals: Networks, global topography, and function. *J. Neurophysiol.* **131**, 1014–1082 (2024), 10.1152/jn.00308.2023.
53. R. M. Braga, K. R. A. Van Dijk, J. R. Polimeni, M. C. Eldaief, R. L. Buckner, Parallel distributed networks resolved at high resolution reveal close juxtaposition of distinct regions. *J. Neurophysiol.* **121**, 1513–1534 (2019).
54. D. Reznik, R. Trampel, N. Weiskopf, M. P. Witter, C. F. Doeller, Dissociating distinct cortical networks associated with subregions of the human medial temporal lobe using precision neuroimaging. *Neuron* **111**, 2756-2772.e7 (2023), 10.1016/j.neuron.2023.05.029.
55. A. W. Gilmore, S. M. Nelson, K. B. McDermott, A parietal memory network revealed by multiple MRI methods. *Trends Cogn. Sci.* **19**, 534–543 (2015).
56. W. W. Seeley, The salience network: A neural system for perceiving and responding to homeostatic demands. *J. Neurosci.* **39**, 9878–9882 (2019).
57. W. W. Seeley *et al.*, Dissociable intrinsic connectivity networks for salience processing and executive control. *J. Neurosci.* **27**, 2349–2356 (2007).
58. E. T. Rolls *et al.*, Hippocampal neurons in the monkey with activity related to the place in which a stimulus is shown. *J. Neurosci.* **9**, 1835–1845 (1989).
59. R. T. Knight, Contribution of human hippocampal region to novelty detection. *Nature* **383**, 256–259 (1996).
60. M. Fyhn, S. Molden, S. Hollup, M.-B. Moser, E. I. Moser, Hippocampal neurons responding to first-time dislocation of a target object. *Neuron* **35**, 555–566 (2002).
61. D. Kumaran, E. A. Maguire, Novelty signals: A window into hippocampal information processing. *Trends Cogn. Sci.* **13**, 47–54 (2009).
62. N. U. F. Dosenbach *et al.*, A core system for the implementation of task sets. *Neuron* **50**, 799–812 (2006).
63. M. D. Fox, A. Z. Snyder, D. M. Barch, D. A. Gusnard, M. E. Raichle, Transient BOLD responses at block transitions. *Neuroimage* **28**, 956–966 (2005).
64. S. Konishi, D. I. Donaldson, R. L. Buckner, Transient activation during block transition. *Neuroimage* **13**, 364–374 (2001).
65. L. Litman, J. Robinson, T. Abberbock, TurkPrime.com: A versatile crowdsourcing data acquisition platform for the behavioral sciences. *Behav. Res. Methods* **49**, 433–442 (2017).
66. R. M. Braga, R. L. Buckner, Parallel interdigitated distributed networks within the individual estimated by intrinsic functional connectivity. *Neuron* **95**, 457–471.e5 (2017).
67. R. Kong *et al.*, Spatial topography of individual-specific cortical networks predicts human cognition, personality, and emotion. *Cereb. Cortex* **29**, 2533–2551 (2019).
68. B. Fischl *et al.*, Whole brain segmentation: Automated labeling of neuroanatomical structures in the human brain. *Neuron* **33**, 341–355 (2002).
69. B. Fischl *et al.*, Sequence-independent segmentation of magnetic resonance images. *Neuroimage* **23**, S69–S84 (2004).
70. H. L. Kosakowski, N. Saadon-Grosman, J. Du, M. C. Eldaief, R. L. Buckner, Human Striatal Association Megaclusters. *J. Neurophysiol.* **131**, 1083–1100 (2024), 10.1152/jn.00387.2023.
71. M. F. Glasser *et al.*, The minimal preprocessing pipelines for the human connectome project. *Neuroimage* **80**, 105–124 (2013).
72. D. Marcus *et al.*, Informatics and data mining tools and strategies for the human connectome project. *Front Neuroinform.* **5**, 3389 (2011).
73. J. K. Wynn *et al.*, Impaired target detection in schizophrenia and the ventral attentional network: Findings from a joint event-related potential–functional MRI analysis. *Neuroimage Clin* **9**, 95–102 (2015).
74. M. W. Woolrich, B. D. Ripley, M. Brady, S. M. Smith, Temporal autocorrelation in univariate linear modeling of fMRI data. *Neuroimage* **14**, 1370–1386 (2001).
75. S. M. Smith *et al.*, Advances in functional and structural MR image analysis and implementation as FSL. *Neuroimage* **23**, S208–S219 (2004).
76. R. M. Braga, L. M. DiNicola, H. C. Becker, R. L. Buckner, Situating the left-lateralized language network in the broader organization of multiple specialized large-scale distributed networks. *J. Neurophysiol.* **124**, 1415–1448 (2020).
77. N. Saadon-Grosman *et al.*, Within-individual organization of the human cognitive cerebellum: Evidence for closely juxtaposed, functionally specialized regions. *Sci. Adv.* **10**, eadq4037 (2024).
78. D. Hassabis, E. A. Maguire, The construction system of the brain. *Philos. Trans. R Soc. Lond B Biol. Sci.* **364**, 1263–1271 (2009).
79. C. E. L. Stark, L. R. Squire, When zero is not zero: The problem of ambiguous baseline conditions in fMRI. *Proc. Natl. Acad. Sci. U.S.A.* **98**, 12760–12766 (2001).
80. R. L. Buckner, L. M. DiNicola, The brain's default network: Updated anatomy, physiology and evolving insights. *Nat. Rev. Neurosci.* **20**, 593–608 (2019).
81. M. A. Dalton, P. Zeidman, C. McCormick, E. A. Maguire, Differentiable processing of objects, associations, and scenes within the hippocampus. *J. Neurosci.* **38**, 8146–8159 (2018).
82. P. Leelaarporn *et al.*, Hippocampal subfields and their neocortical interactions during autobiographical memory. *Imaging Neurosci.* **2**, 1–13 (2024).
83. A. W. Gilmore *et al.*, Evidence supporting a time-limited hippocampal role in retrieving autobiographical memories. *Proc. Natl. Acad. Sci. U.S.A.* **118**, e2023069118 (2021).
84. S. Audrain, A. W. Gilmore, J. M. Wilson, D. L. Schacter, A. Martin, A role for the anterior hippocampus in autobiographical memory construction regardless of temporal distance. *J. Neurosci.* **42**, 6445–6452 (2022).
85. S. M. Nelson, K. M. Arnold, A. W. Gilmore, K. B. McDermott, Neural signatures of test-potentiated learning in parietal cortex. *J. Neurosci.* **33**, 11754–11762 (2013).
86. H.-Y. Chen, A. W. Gilmore, S. M. Nelson, K. B. McDermott, Are there multiple kinds of episodic memory? An fMRI investigation comparing autobiographical and recognition memory tasks *J. Neurosci.* **37**, 2764–2775 (2017).
87. A. Ben-Yakov, Y. Dudai, Constructing realistic engrams: Poststimulus activity of hippocampus and dorsal striatum predicts subsequent episodic memory. *J. Neurosci.* **31**, 9032–9042 (2011).
88. C. Baldassano *et al.*, Discovering event structure in continuous narrative perception and memory. *Neuron* **95**, 709–721.e5 (2017).
89. A. Ben-Yakov, R. N. Henson, Eds., The hippocampal film editor: Sensitivity and specificity to event boundaries in continuous experience. *J. Neurosci.* **38**, 10057–10068 (2018).
90. Z. M. Reagh, A. I. Delarazan, A. Garber, C. Ranganath, Aging alters neural activity at event boundaries in the hippocampus and posterior medial network. *Nat. Commun.* **11**, 3980 (2020).
91. A. J. Barnett *et al.*, Hippocampal-cortical interactions during event boundaries support retention of complex narrative events. *Neuron* **112**, 319–330.e7 (2024).
92. J. M. Zacks, N. K. Speer, K. M. Swallow, T. S. Braver, J. R. Reynolds, Event perception: A mind-brain perspective. *Psychol. Bull.* **133**, 273 (2007).
93. J. C. R. Whittington *et al.*, The tolman-eichenbaum machine: Unifying space and relational memory through generalization in the hippocampal formation. *Cell* **183**, 1249–1263.e23 (2020).
94. Y. Kwon *et al.* Situating the parietal memory network in the context of multiple parallel distributed networks using high-resolution functional connectivity. bioRxiv [Preprint] (2023). https://www.biorxiv.org/content/10.1101/2023.08.16.553585v1 (Accessed 15 November 2023).
95. A. W. Gilmore *et al.*, High-fidelity mapping of repetition-related changes in the parietal memory network. *Neuroimage* **199**, 427–439 (2019).
96. B. J. Shannon, R. L. Buckner, Functional–anatomic correlates of memory retrieval that suggest nontraditional processing roles for multiple distinct regions within posterior parietal cortex. *J. Neurosci.* **24**, 10084–10092 (2004).